Theoretical analysis of polarization control for the stable output of multi-carrier source based on a re-circulating frequency shifter

Hao Zhou (周 浩), Lixia Xi (席丽霞), Jianping Li (李建平), Xiaoguang Zhang (张晓光)*, and Na Liu (刘 娜)

State Key Laboratory of Information Photonics and Optical Communications, Beijing University of Posts and Telecommunications, Beijing 100876, China

**Corresponding author: xgzhang@bupt.edu.cn*

Received January 13, 2012; accepted April 13, 2012; posted online August 3, 2012

Fluctuating polarization state-of-light in the optical loop is an important factor that seriously influences the output performance of a multi-carrier source based on re-circulating frequency shifter (RFS). The reason for output spectrum instability when no polarization controller (PC) is present in the loop is analyzed theoretically. Numerical simulations for the output spectra of the multi-carrier source with and without PC are conducted, and the trajectories of the several frequency components polarization states on the Poincare sphere with and without PC are compared. The results show that the performance of multi-carrier source based on a RFS can be improved effectively by adjusting the PC in the configuration properly.

OCIS codes: 060.2330, 060.2630, 230.5440.

doi: 10.3788/COL201210.100602.

In order to meet increasing demand for the capacity and transmission efficiency of the communication system, many frontier studies on single-source Tb/s transmission have been conducted[1−5]. Coherent optical orthogonal-frequency-division-multiplexing (CO-OFDM)[1−3] and coherent wavelength-division-multiplexing (CO-WDM)[4,5] systems based on a single-laser source have been widely applied in several Tb/s rate transmission experiments wherein a multi-carrier source is required. Several structures of multi-carrier sources have been identified, including the optical frequency comb technique[6], the multi-wavelength erbium-doped fiber laser (EDFL)[7], the cascaded phase modulator and the intensity modulator[8], two cascaded phase modulators based on re-circulating frequency shifter (RFS)[9], the multi-frequency phase modulator[10], and single-sideband (SSB) modulator based on RFS[11]. Compared with other methods, the SSB modulator based on RFS has many advantages, such as low driving voltage and controllable output frequency range, carrier interval, and carrier numbers. However, because of the polarization sensitive characteristics of the I/Q modulator, the SSB multi-carrier source is easily influenced by changes in the laser polarization state[12]. Therefore, determining how the polarization state-of-light influences the output of multi-carrier source and how to control the polarization state to realize output stability is important.

In this letter, we theoretically analyze the change of the polarization state when optical signals pass through I/Q modulator, as well as the reason for the output instability of the multi-carrier source. Numerical simulations on the output spectra of multi-carrier generation system with and without a polarization controller (PC) are conducted, and the polarization states of each frequency component after every circulation are shown using a Poincare sphere. Stable output of the multi-carrier source can be realized by adjusting PC properly.

The diagram of the multi-carrier generator based on RFS is shown in Fig. 1. This generator is a closed-loop system that consists of a CW laser, a 50:50 coupler, an I/Q modulator, an optical band-pass filter (OBPF), an optical amplifier (OA), and a PC. In this structure, the CW laser is used as the seed light source, the OBPF is used to control the number of carriers, the OA is to compensate for the modulation and insertion losses, and the PC is used to control polarization state of the light.

The I/Q modulator consists of two Mach-Zenhder modulators (MZMs) placed parallel in two arms, and a $\pi/2$-phase shifter in one arm. The I/Q modulator is driven by three DC voltages and two equal-amplitude but $\pi/2$-phase shifted radio frequency (RF) clock signals through the I and Q ports. The I/Q modulator is a polarization-sensitive device; thus, it will modulate light oriented along one polarization while leaving the light polarized orthogonal to this orientation unchanged[13]. The polarization state of the output light of the I/Q modulator will experience random changes when the light is transmitted into the circulation loop. Thus, each time the light passes the I/Q modulator, some light components will not be modulated. These unmodulated components finally destroy the stability of the output spectrum. Next, the theoretical derivation based on one component is discussed.

Assuming one component of input light of the I/Q modulator, expressed as a Jones vector, is

$$\mathbf{E}_{\text{in}} = \begin{bmatrix} E_x e^{j(\omega_n t)} \\ E_y e^{j(\omega_n t + \Delta\theta_{xy})} \end{bmatrix}, \tag{1}$$

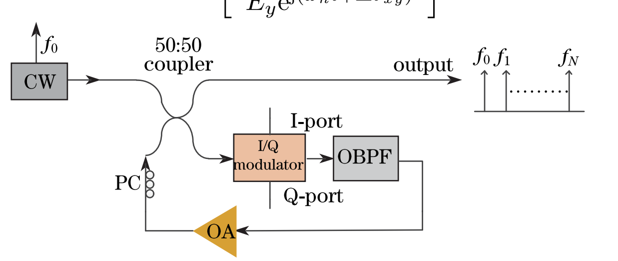

Fig. 1. Diagram of the multi-carrier generator based on RFS.

where E_x and E_y stand for the amplitude of the light in the x and y polarization components, respectively; $\Delta\theta_{xy}$ is the phase difference between them; ω_n stands for radian frequency of the input light (center frequency f_n). The operational drive signals of the I/Q modulator are $S_{\mathrm{I}}(t) = V_\pi + V_{\mathrm{RF}}\cos(2\pi f_m t)$, $S_{\mathrm{Q}}(t) = V_\pi + V_{\mathrm{RF}}\sin(2\pi f_m t)$, and $S_{\mathrm{PM}}(t) = V_{\pi\mathrm{PM}}$, where V_π and $V_{\pi\mathrm{PM}}$ stand for the half-wave voltage of the MZM and phase modulator, respectively, f_m is the frequency shift of the multi-carrier (radian frequency ω_m), and V_{RF} is the amplitude of RF signal. Here, we define the quantity $\delta = (\pi V_{\mathrm{RF}})/(2V\pi)$, which stands for the modulation depth. Assuming the I/Q modulator only modulates light polarizing in the x direction, we can obtain the output of the two branches of the I/Q modulator by means of the Jacobi-Anger expansion:

$$\mathbf{E}_{\mathrm{I}} = \frac{1}{2\sqrt{2}}\begin{bmatrix} E_x \mathrm{e}^{\mathrm{j}(\omega_n t - \frac{\pi}{2})} \cdot \sum\limits_{n=-\infty}^{\infty} (-\mathrm{j})^n J_n(\delta)\mathrm{e}^{\mathrm{j}n\omega_m t} \\ E_y \mathrm{e}^{\mathrm{j}(\omega_n t + \Delta\theta_{xy})} \end{bmatrix} + \frac{1}{2\sqrt{2}}\begin{bmatrix} E_x \mathrm{e}^{\mathrm{j}(\omega_n t + \frac{\pi}{2})} \cdot \sum\limits_{n=-\infty}^{\infty} \mathrm{j}^n J_n(\delta)\mathrm{e}^{\mathrm{j}n\omega_m t} \\ E_y \mathrm{e}^{\mathrm{j}(\omega_n t + \Delta\theta_{xy})} \end{bmatrix}, \quad (2)$$

$$\mathbf{E}_{\mathrm{Q}} = \frac{1}{2\sqrt{2}}\begin{bmatrix} E_x \mathrm{e}^{\mathrm{j}\omega_n t} \cdot \sum\limits_{n=-\infty}^{\infty} (-1)^n J_n(\delta)\mathrm{e}^{\mathrm{j}n\omega_m t} \\ E_y \mathrm{e}^{\mathrm{j}(\omega_n t + \Delta\theta_{xy})} \end{bmatrix} + \frac{1}{2\sqrt{2}}\begin{bmatrix} E_x \mathrm{e}^{\mathrm{j}(\omega_n t + \pi)} \cdot \sum\limits_{n=-\infty}^{\infty} J_n(\delta)\mathrm{e}^{\mathrm{j}n\omega_m t} \\ E_y \mathrm{e}^{\mathrm{j}(\omega_n t + \Delta\theta_{xy})} \end{bmatrix}. \quad (3)$$

Neglecting all the harmonics beyond the 3rd-order in Eqs. (2) and (3), the output of the I/Q modulator would be

$$\mathbf{E}_{\mathrm{out}} = \begin{bmatrix} -E_x J_1(\delta)\cos[2\pi(f_n + f_m)t] \\ 0 \end{bmatrix} + \begin{bmatrix} 0 \\ E_y \cos(2\pi f_n t + \Delta\theta_{xy}) \end{bmatrix} + \begin{bmatrix} E_x J_3(\delta)\cos[2\pi(f_n - 3f_m)t] \\ 0 \end{bmatrix}. \quad (4)$$

This process is illustrated in Fig. 2 (only the 0th and 1st harmonics are displayed).

The computational analysis above implies that whether or not the input light can be modulated completely (the completeness of input light modulation) has a significant effect on the stability of the output spectrum. If we wish the input light to be modulated completely, we should adjust the polarization state of the input light align with that of the I/Q modulator.

A wave-plate-type PC is used to change the polarization state of the light. The diagram of the PC is shown in Fig. 3. This PC consists of one 1/2 wave plate and two 1/4 wave plates, the retardation of which are fixed and fast-axis orientation angles are changeable. In the following simulation, we hope to change the input elliptically polarized light to linearly polarized light by the first 1/4 wave plate, adjust the 1/2 wave plate to obtain linearly polarized light (1,0,0), and, finally, place the fast axis of the second 1/4 wave plate along the x axis. The fast-axis orientation angles of the three wave plates are satisfied with

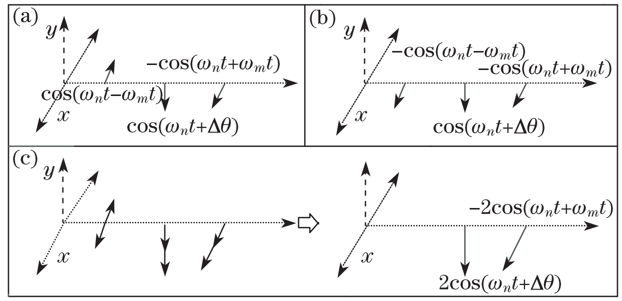

Fig. 2. Frequency spectra of the modulation in (a) one and (b) the other branchs; (c) frequency spectrum after I/Q modulator.

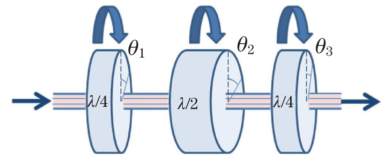

Fig. 3. Diagram of the PC.

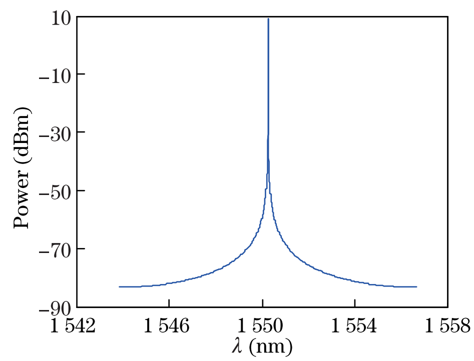

Fig. 4. Frequency spectrum of the input laser.

$$2\theta_1 = 2\theta_{\mathrm{in}}, \quad (5)$$

$$2\theta_2 = \theta_{\mathrm{in}} + \varepsilon_{\mathrm{in}} + \theta_{\mathrm{out}} - \varepsilon_{\mathrm{out}}, \quad (6)$$

$$2\theta_3 = 2\theta_{\mathrm{out}}, \quad (7)$$

where θ_1, θ_2, and θ_3 stand for fast-axis orientation angle of the three wave plates, respectively; θ_{in} and $\varepsilon_{\mathrm{in}}$ stand for azimuth angle and ellipticity, respectively, of the input polarization state; θ_{out} and $\varepsilon_{\mathrm{out}}$ stand for azimuth angle and ellipticity, respectively, of the output polarization state which we want to obtain.

In the simulation, we set the following conditions: power of the CW laser as 12 dBm, center wavelength of the output laser as 1 550.268 nm (f_0 =193.577 THz), polarization state $\mathbf{E}_{\mathrm{CW}} = \frac{E_0}{\sqrt{2}}\begin{bmatrix} \mathrm{e}^{\mathrm{j}2\pi f_0 t} \\ 0 \end{bmatrix}$ (the polarization direction of the input light and the modulation direction of the I/Q modulator are parallel), carrier frequency interval $f_m = 12.5$ GHz, and modulation depth $\delta = 0.65$. Assuming that the OBPF covers the range from f_0 to $f_0 + 14f_m$ for generating 15 carriers and that the saturation output power of the Raman amplifier is 21.26 dBm, the spectrum of the input laser is shown in Fig. 4.

We first simulate the output spectra of the multi-carrier generation system without PC, as shown in Fig. 5. Clearly, the spectra differ for different circulation numbers. In other words, performance of the multi-carrier source is unstable. The polarization states of some frequency components after each circulation (18 circulations altogether) are shown using a Poincare sphere in

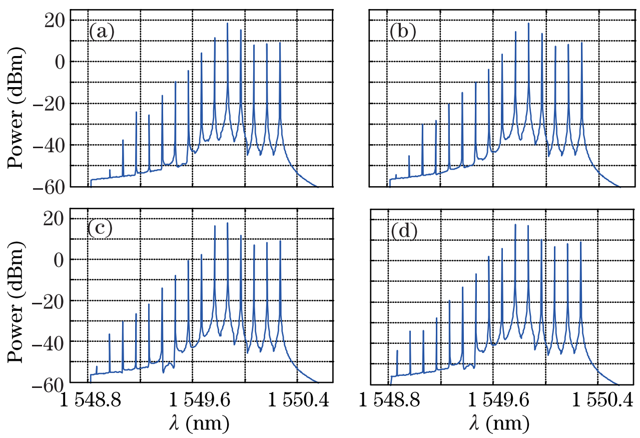

Fig. 5. Output spectra of the system without PC: (a) 15, (b) 16, (c) 17, and (d) 18 circulations.

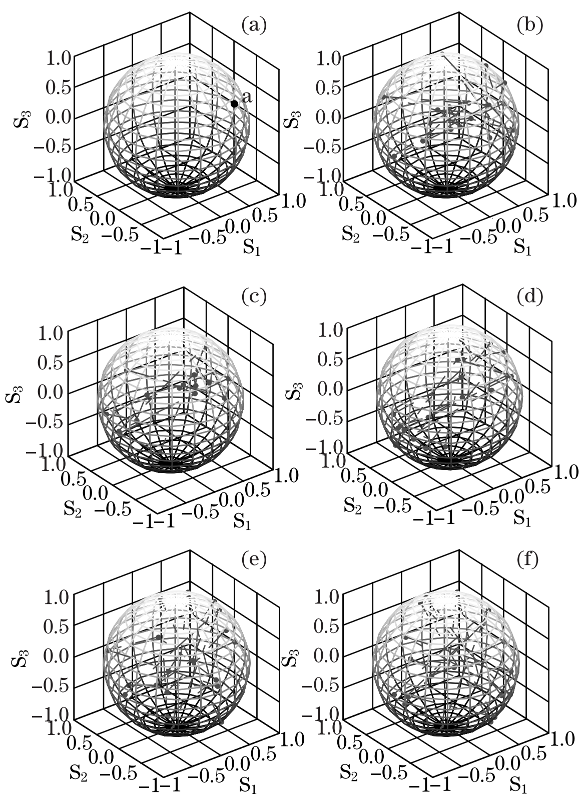

Fig. 6. Polarization states of some frequency components after every circulation (18 circulations): (a) seed laser; (b) f_0+f_m; (c) f_0+4f_m; (d) f_0+7f_m; (e) f_0+10f_m; (f) f_0+13f_m.

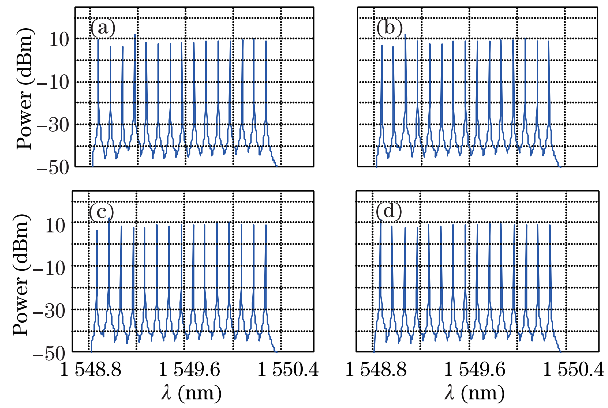

Fig. 7. Output spectra of the system with PC: (a) 15, (b) 16, (c) 17, and (d) 18 circulations.

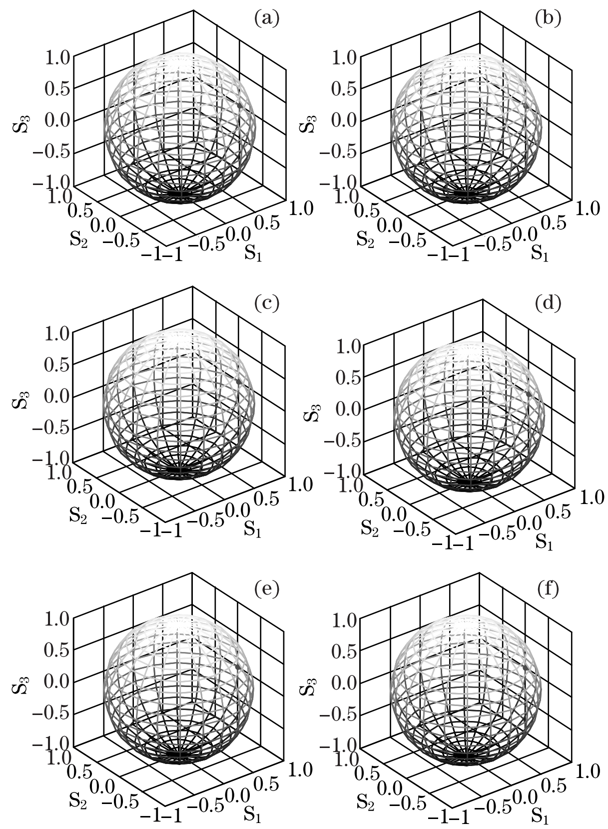

Fig. 8. Polarization states of some frequency components after every circulation (18 circulations): (a) seed laser; (b) f_0+f_m; (c) f_0+4f_m; (d) f_0+7f_m; (e) f_0+10f_m; (f) f_0+13f_m.

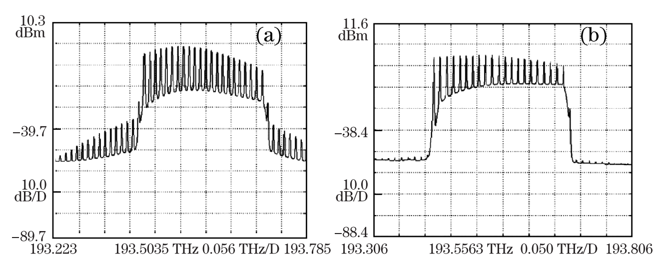

Fig. 9. Experimental result of the multi-carrier generation system (a) without and (b) with polarization control.

Fig. 6, where the point "a" stands for polarization state of the seed laser. The polarization state of each component varies largely with each circulation and seems to be disordered. The simulation results are in accordance with the theoretical derivation.

With the addition of PC in the simulation system and by adjusting the fast-axis angle of the three wave plates using Eqs. (5)–(7), stable and flat multi-carrier output spectra can be obtained. In addition, the azimuth angle and ellipticity of the PC's input light can be calculated using the position of the point shown in the Poincare sphere that represents the polarization state of $f_0 + f_m$ frequency component in the first circulation. The desired azimuth angle and ellipticity of the output polarization state are same that as of the input CW laser (in order to be modulated completely by the I/Q modulator). Figures 7 and 8 show the simulation results of the system with PC in the loop. By adjusting the PC, the polarization states of each frequency component will arrive at point (1,0,0) after every circulation. Then, flat and stable output spectra can be realized.

Several experiments were carried out to preliminarily validate the simulation result. The experimental results of the multi-carrier generation system with and without PC are shown in Fig. 9. The output spectra of the multi-carrier generation system were influenced, not only by PC, but also by the performance of some components, such as the OA, the OBPF, and the optical fiber.

In conclusion, we theoretically analyze the instability of the multi-carrier source outputs induced by random changes in the signal polarization states and solve the issue of instability by adding PC in the loop. The effectiveness of our method by comparing the output spectra of the multi-carrier generation system with and without PC by simulations is demonstrated, as well as by varying of the signal polarization states shown in the Poincare sphere. The results indicate that, by adjusting the azimuth angle of the PC, the multi-carrier output performance can be improved. Our research can provide an important theoretical guide to improve multi-carrier output quality, and pave the way for SSB multi-carrier generation based on RFS to be used in next generation Terabit communication system.

This work was supported by the Chinese Universities Scientific Fund (No. BUPT 2011RC009), the BUPT Excellent Ph.D. Students Foundation (No. CX201121), and the Research Fund for the Doctoral Program of Higher Education (No. 20110005110014).

References

1. Y. Ma, Q. Yang, Y. Tang, S. Chen, and W. Shieh, in *Proceedings* of *OFC* 2009 PDPC1 (2009).
2. B. Zhu, X. Liu, S. Chandrasekhar, D. W. Peckham, and R. Lingle, IEEE Photon. Technol. Lett. **22,** 826 (2010).
3. X. Liu, S. Chandrasekhar, B. Zhu, and D. W. Peckham, in *Proceedings of OFC 2010* OWO2 (2010).
4. A. D. Ellis, F. C. G. Gunning, B. Cuenot, T. C. Healy, and E. Pincemin, in *Proceedings of OECC 2008* WeA-1 (2008).
5. G. Gavioli, E. Torrengo, G. Bosco, A. Carena, S. J. Savory, F. Forghieri, and P. Poggiolini, IEEE Photon. Technol. Lett. **22,** 1419 (2010).
6. T. Sakamoto, T. Yamamoto, K. Kurokawa, and S. Tomita, Electron. Lett. **45,** 850 (2009).
7. M. A. Mirza and G. Stewart, J. Lightwave Technol. **27,** 1034 (2009).
8. J. Yu, X. Zhou, M. Huang, D. Qian, P. N. Ji, T. Wang, and P. Magill, Opt. Express **17,** 17928 (2009).
9. J. Zhang, N. Chi, J. Yu, Y. Shao , J. Zhu, B. Huang, and L. Tao, Opt. Express **19,** 12891 (2011).
10. Y. Lu, Y. Xing, and Y. Dong, Chin. Opt. Lett. **8,** 316 (2010).
11. J. Li, X. Li, X. Zhang, F. Tian, and L. Xi, Opt. Express **18,** 17597 (2010).
12. F. Tian, X. Zhang, J. Li, and L. Xi, Chin. Phys. Lett. **27,** 094206 (2010).
13. A. L. Campillo, IEEE Photon. Technol. Lett. **18,** 1780 (2006).